High-resolution monochromatized He II α-excited photoelectron spectrum of Ar between 28 and 40.8 eV

M. Lundqvist, P. Baltzer, L. Karlsson, and B. Wannberg
Department of Physics, Uppsala University, Box 530, S-751 21 Uppsala, Sweden
(Received 29 September 1992; revised manuscript received 6 July 1993)

The inner-valence-photoelectron spectrum of argon has been recorded between 28 and 40.8 eV at a resolution of 20 meV using monochromatized He II α excitation. More than 40 lines are observed and assigned by comparison to optical data and theoretical results. Except for the 3*s* single-hole state at 29.240 eV, the spectrum is associated with transitions to electron-correlation states arising from $3p^4\,nl$ configurations, where $n=3,4,5$ and $l=0$–3. The complete manifold of ionic states is observed for most configurations. Final states with an angular momentum up to $J=\frac{9}{2}$ acquire a substantial intensity.

PACS number(s): 32.80.Fb, 32.70.Fw

I. INTRODUCTION

The inner-valence-photoelectron spectrum of argon has previously been recorded using Al $K\alpha$ radiation (XPS) [1] and synchrotron radiation [2–8]. A number of lines associated with shake-up and correlation states have been observed in addition to the single line expected for the 3*s* ionization. These results are important for a good understanding of the photoionization dynamics and have formed a basis for the development of theoretical methods.

The XPS studies were carried out at a resolution of about 0.4 eV and six lines could be resolved in the binding-energy region between 30 and 40 eV. However, from optical data [9,10] it is clear that additional lines should appear in more highly resolved spectra. Such studies have been carried out using synchrotron radiation at a resolution of about 50 meV [2,4], 70 meV [3], 100 meV [5], 0.16 eV [6], and 0.3 eV [7,8]. In Refs. [1,4,6–8] relative intensities are reported for the main line and a number of satellites, while the other studies concentrate on the energies and threshold effects. Additional detailed and complementary information concerning the significance of correlation effects in the photoionization process has been obtained from fluorescence spectroscopy in the wavelength region between 400 and 780 Å at a resolution between 50 and 100 meV [11].

A number of theoretical studies have been reported which consider configuration interaction in both the initial state and final states [12–18]. Most of these either concern the experimental situation prevailing at higher energies than that used in the present study or consider only earlier low-resolution recordings.

In the present investigation we have recorded photoelectron spectra using monochromatized He II α radiation at a resolution of 20 meV. Detailed assignments are made by comparison to optical data and theoretical considerations. Relative intensities are obtained in the entire energy region up to 40.8 eV. These are important in order to determine the significance of the various correlation effects in the photoionization process.

II. EXPERIMENTAL DETAILS

The spectra were recorded on a uv photoelectron spectrometer of the hemispherical analyzer type with a mean radius of 144 mm. This instrument has been described elsewhere [19]. The He resonance radiation was obtained from a microwave-driven ECR source [20,21] using a He gas pressure of about 50 mtorr. The discharge produces He I radiation, which is about 20 times more intense than the He II components. Unless this low-energy radiation is eliminated or strongly reduced, inner-valence studies in the range between 30 and 40 eV are practically impossible. In the present investigation we have employed a toroidal grating monochromator [22] to focus the He II α radiation and eliminate other lines. Due to stray light from the grating, a flux of He I radiation remains, with an intensity of 10^{-4}–10^{-3} of the original. In spite of this reduction, the He I excited Ar 3*p* lines still dominate the spectrum, but the background of scattered electrons is sufficiently low so as not to disturb the satellite spectrum significantly. The analyzer pass energy was 20 eV in all recordings and the steplength was 5 meV except in the recording of Fig. 1 where 10 meV was used. The spectra were energy calibrated against the Ar $3p_{1/2,3/2}$ lines generated by the He I radiation, with binding energies of 15.937 and 15.759 eV, respectively [9].

All spectra were obtained by recording photoelectrons that leave the sample gas at 90° from the direction of the photon beam, and the radiation was unpolarized. The gas pressure was kept sufficiently low, on the order of 10 mtorr, to prevent inelastic scattering peaks to appear with measurable intensity. The spectra presented in this report are displayed exactly as they were recorded, without any background subtraction or deconvolution. Line positions and relative intensities were obtained from curve fits using Gaussians to represent the spectrometer function. The line position has been taken as the center of the corresponding Gaussian and the intensity as its area. The probable error limits are less than 2 meV and a few percent, respectively, in these determinations. The sample gas was commercially obtained with a stated puri-

1050-2947/94/49(1)/277(6)/$06.00

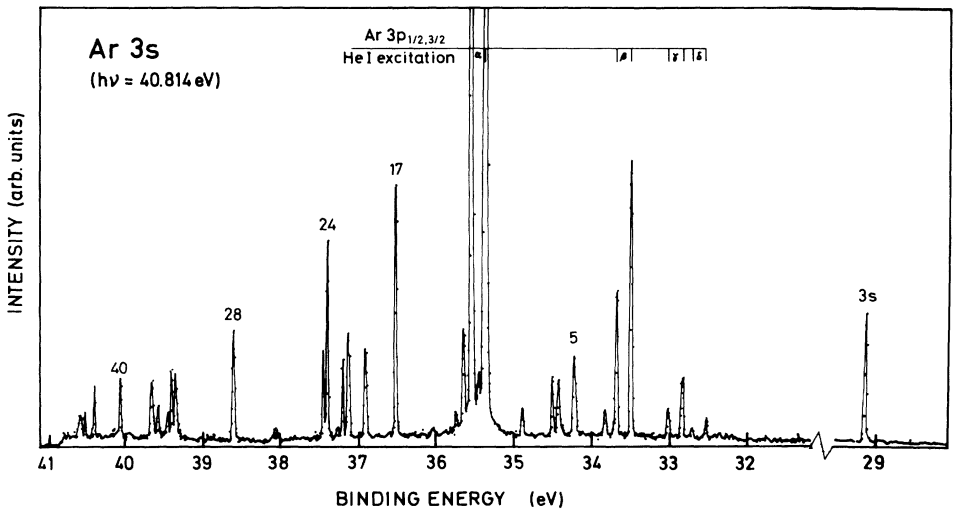

FIG. 1. The inner-valence-photoelectron spectrum of Ar between 28 and 41 eV excited by means of monochromatized He II α radiation at 40.814 eV. The Ar $3p$ lines appear in the spectrum due to some remaining He I radiation. Excitation with the He I α, β, γ, and δ components are indicated.

ty of better than 99.9996%.

In order to obtain the correct relative intensities over the total spectrum, which covers a range of kinetic energies (E_K) from about 0.5 to 12 eV, the spectra should be corrected for the transmission function of the spectrometer. Since this is not known with any certainty, we have not attempted any such correction. Thus, intensity comparisons are only relevant for lines that are close in kinetic energy. From considerations of the electron optics, it can be expected that the transmission should vary as E_K^{-p}, where p is not too far from 0.5, except at the very lowest kinetic energies, where the transmission should be more or less constant.

III. RESULTS

Figure 1 shows the complete spectrum including the $3s$ line at 29.240 eV and the satellite region up to 40.814 eV. The background is essentially constant over the spectrum and decreases in an obvious manner at the ionization limit. The series of lines corresponding to the Ar $3p_{1/2,3/2}$ ionization by residual He I radiation can be easily identified. Lines induced by the four first components are clearly seen in this spectrum, and even higher components can be observed in more detailed spectra in the 32-eV range. A total of 47 lines, which can be associated with correlation states, have been observed in this spectrum. These are listed in Table I. The assignments have been made by comparisons to data from optical spectroscopy and calculations. The spectrum is partly quite complex and therefore needs more detailed consideration, which is given in the following.

The first two satellite lines occur at 33.702 and 33.821 eV (cf. Fig. 2) and can be associated with the $3p^4(^3P)3d\ ^2P_{1/2,3/2}$ ionic states. The apparent absence of lines at lower energies is in agreement with spectra obtained previously using synchrotron radiation in the 40–80-eV range [3,4,7,8]. In threshold photoelectron spectra, a number of lines observed in this range [2,3] can probably be related to the presence of resonance states

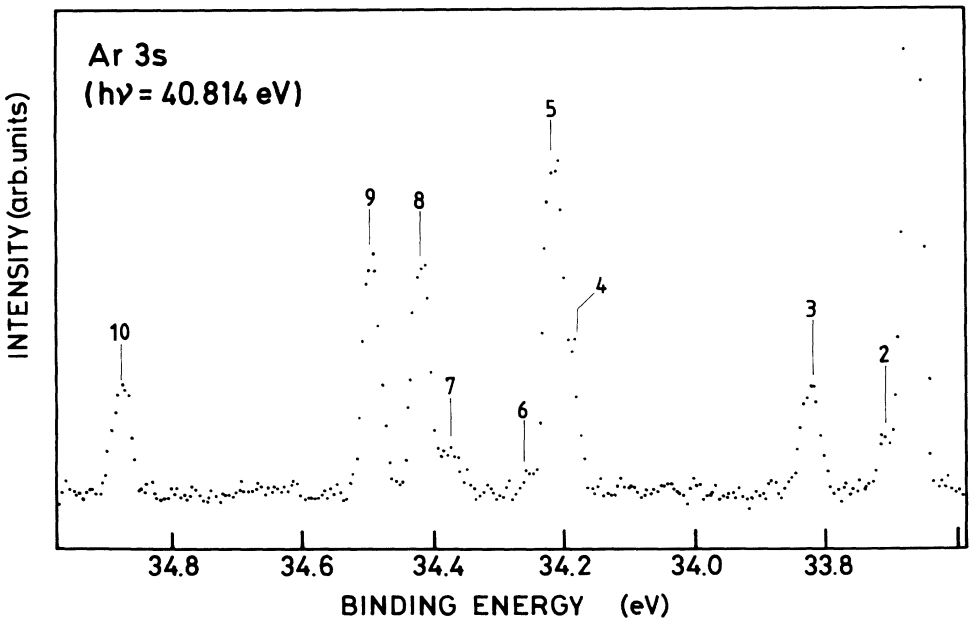

FIG. 2. An enlarged part of the inner-valence satellite spectrum of argon showing the region between 33.6 and 35 eV.

[23] in the excitation energy region. Another eight lines can be seen in the range up to 35 eV. They can be associated with transitions to many-electron states with ^2P, ^2D, ^2F, and even ^2G symmetry (cf. Table I). Due to their weakness, the relative intensities of lines 6 and 7 given in Table I are somewhat uncertain, whereas the other lines are well determined.

In the 35- to 36-eV range there is a strong overlap with the Ar $3p_{1/2,3/2}$ lines excited by the residual He I radiation. However, four lines are well resolved and two are partly resolved (12 and 13). They correspond well to the transitions expected in this region. The next line (16) observed slightly above 36 eV is weak and broad (cf. Fig. 1). It can be ascribed to the $3p^4(^1D)3d\ ^2F_{7/2,5/2}$ spin-orbit split states expected at 36.006 and 36.032 eV, respectively. The line is clearly asymmetric, with the highest intensity on the high-binding-energy side. This indicates an inverted ordering of the spin-orbit split components, compared to the other states of this $3p^4(^1D)3d$ configuration, which is consistent with results of optical spectroscopy. The energies and relative intensities of the transitions given in Table I give a very good fitting to the observed line.

The energy range between 36.4 and 37.5 eV contains a group of lines that is shown separately in Fig. 3. The second and fifth of these lines are clearly asymmetric in the figure and are indicated as doublets, 18, 19 and 22, 23, respectively. Even line 20 shows a slight asymmetry, suggesting that both spin-orbit split components $3p^4(^1D)4p\ ^2P_{3/2}$ and $3p^4(^1D)3d\ ^2D_{5/2}$ expected at this energy provide some intensity. The relative intensities presented in Table I were obtained by a curve fitting analysis of this line. Assuming that the statistical ratios between the spin-orbit split components are reflected in line 21, the intensity ratio between the $3p^4(^1D)4p\ ^2P$ and $3p^4(^1D)3d\ ^2D$ states, which has been much discussed in earlier studies [16–18], is obtained. The present data indicate that at 40.8 eV the intensity of the latter is somewhat larger.

Lines 26 and 27 are weak but easily observed in the

TABLE I. Binding energies, relative intensities (peak areas), and assignments of the peaks observed in the inner-valence region of argon between 29 and 40.8 eV. The intensities have been normalized to 10 000 for the most intense line at 36.504 eV. Intensities which have been inferred from statistical ratios are denoted by an asterisk (*). For the $3p^44f$ states $J_c l$ coupling is appropriate and the corresponding quantum number is given in square brackets (Ref. [10]).

Peak number	Binding energy (eV)	Relative peak area	Assignment	Peak number	Binding energy (eV)	Relative peak area	Assignment
1	29.240	5100	$3s3p^6\ ^2S_{1/2}$	31	39.309	740*	$3p^4(^3P)4d\ ^2P_{1/2}$
2	33.702	640	$3p^4(^3P)3d\ ^2P_{1/2}$	31	39.330	1600*	$3p^4(^3P)5p\ ^2P^o_{3/2}$
3	33.821	1300	$3p^4(^3P)3d\ ^2P_{3/2}$	31	39.341	790*	$3p^4(^3P)5p\ ^2P^o_{1/2}$
4	34.187	1400	$3p^4(^1D)4s\ ^2D_{3/2}$	32	39.380	1100*	$3p^4(^3P)5p\ ^2D^o_{5/2}$
5	34.214	3400	$3p^4(^1D)4s\ ^2D_{5/2}$	32	39.391	1500*	$3p^4(^3P)4d\ ^2P_{3/2}$
6	34.256	220	$3p^4(^3P)3d\ ^2F_{7/2}$	33	39.434	230	$3p^4(^3P)5p\ ^2S^o_{1/2}$
7	34.376	450	$3p^4(^3P)3d\ ^2F_{5/2}$	33	39.442	750*	$3p^4(^3P)5p\ ^2D^o_{3/2}$
8	34.417	2400	$3p^4(^3P)3d\ ^2D_{3/2}$	34	39.562	1000	$3p^4(^1S)4p\ ^2P^o_{3/2}$
9	34.492	2400	$3p^4(^3P)3d\ ^2D_{5/2}$	35	39.606	500	$3p^4(^1S)4p\ ^2P^o_{1/2}$
10	34.877	1050	$3p^4(^1D)3d\ ^2G_{7/2,9/2}$	36	39.634	1800	$3p^4(^3P)4d\ ^2D_{5/2}$
11	35.440	1300	$3p^4(^3P)4p\ ^2D^o_{5/2}$	37	39.653	1200	$3p^4(^3P)4d\ ^2D_{3/2}$
12	35.522	710*	$3p^4(^3P)4p\ ^2D^o_{3/2}$	38	39.912		$3p^4(^3P_2)4f[4]^o 9/2$
13	35.561	1700*	$3p^4(^3P)4p\ ^2P^o_{1/2}$	38	39.915	210*	$3p^4(^3P_2)4f[4]^o 7/2$
14	35.627	3500	$3p^4(^3P)4p\ ^2P^o_{3/2}$	38	39.920		$3p^4(^3P_2)4f[3]^o 5/2$
15	35.733	660	$3p^4(^3P)4p\ ^2S^o_{1/2}$	38	39.922		$3p^4(^3P_2)4f[3]^o 7/2$
16	36.006	220*	$3p^4(^1D)3d\ ^2F_{5/2}$	39	39.936		$3p^4(^3P_2)4f[2]^o 3/2$
16	36.032	290*	$3p^4(^1D)3d\ ^2F_{7/2}$	39	39.941		$3p^4(^3P_2)4f[2]^o 5/2$
17	36.504	10 000	$3p^4(^1S)4s\ ^2S_{1/2}$	39	39.952	250*	$3p^4(^3P_2)4f[5]^o 11/2$
18	36.887	1900*	$3p^4(^1D)4p\ ^2F^o_{5/2}$	39	39.953		$3p^4(^3P_2)4f[5]^o 9/2$
19	36.903	2500*	$3p^4(^1D)4p\ ^2F^o_{7/2}$	39	39.971		$3p^4(^3P_2)4f[1]^o 1/2$
20	37.112	2500*	$3p^4(^1D)4p\ ^2P^o_{3/2}$	39	39.974		$3p^4(^3P_2)4f[1]^o 3/2$
20	37.127	2600*	$3p^4(^1D)3d\ ^2D_{5/2}$	40	40.044	2000*	$3p^4(^1D)5s\ ^2D_{5/2}$
21	37.187	1200*	$3p^4(^1D)4p\ ^2P^o_{1/2}$	40	40.044		$3p^4(^1D)5s\ ^2D_{3/2}$
21	37.188	1700*	$3p^4(^1D)3d\ ^2D_{3/2}$	41	40.08	390	$3p^4(^3P_1)4f^o_{9/2,\ldots,3/2}$
22	37.252	160*	$3p^4(^1D)4p\ ^2D^o_{3/2}$	42	40.138	230	$3p^4(^3P_0)4f^o_{7/2,5/2}$
23	37.258	250*	$3p^4(^1D)4p\ ^2D^o_{5/2}$	43	40.382	1600*	$3p^4(^1D)4d\ ^2G_{7/2}$
24	37.384	7400	$3p^4(^1D)3d\ ^2P_{3/2}$	43	40.383		$3p^4(^1D)4d\ ^2G_{9/2}$
25	37.435	3500	$3p^4(^1D)3d\ ^2P_{1/2}$	44	40.488	86*	$3p^4(^1D)4d\ ^2P_{1/2}$
26	38.027	540*	$3p^4(^1S)3d\ ^2D_{5/2}$	44	40.498	170*	$3p^4(^1D)4d\ ^2P_{3/2}$
27	38.069	360*	$3p^4(^1S)3d\ ^2D_{3/2}$	45	40.516	750*	$3p^4(^1D)4d\ ^2D_{5/2}$
28	38.585	4000	$3p^4(^1D)3d\ ^2S_{1/2}$	46	40.555	500*	$3p^4(^1D)4d\ ^2D_{3/2}$
29	38.921	250*	$3p^4(^3P)4d\ ^2F_{7/2}$	47	40.573	570*	$3p^4(^1D)4d\ ^2F_{7/2}$
30	39.017	180*	$3p^4(^3P)4d\ ^2F_{5/2}$	48	40.585	430*	$3p^4(^1D)4d\ ^2F_{5/2}$

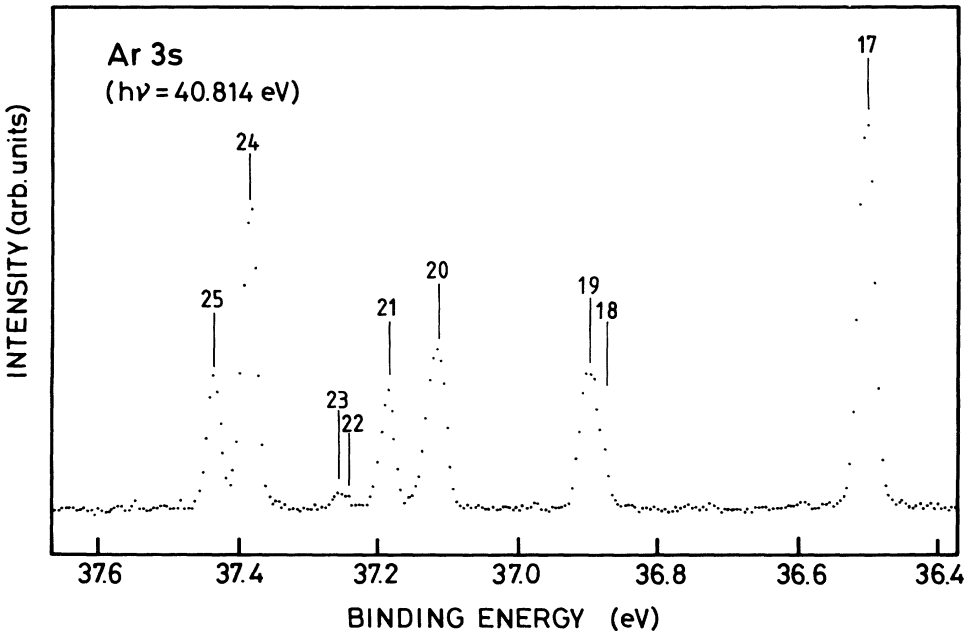

FIG. 3. The He II α excited inner-valence satellite spectrum of argon between 36.4 and 37.6 eV.

otherwise featureless region slightly above 38 eV in Fig. 1. According to Ref. [10] these lines can be associated with the $3p^4(^1S)3d\ ^2D_{3/2,5/2}$ final states, whereas Ref. [9] suggests an assignment in terms of $^2P_{1/2,3/2}$ final states. Although it is not very conclusive, the present study points towards the 2/3 intensity ratio expected for the $^2D_{3/2,5/2}$ states rather than the 1/2 intensity ratio expected for the $^2P_{1/2,3/2}$ final states.

Also lines 29 and 30 at 38.921 and 39.017 eV are weak (cf. Table I). The energies fit exactly with the $3p^4(^1D)4d\ ^2F_{5/2,7/2}$ ionic states, and since no other states are expected at the position of the innermost of these lines, the assignment is straightforward.

In the 39–40-eV range the spectrum is complex due to the presence of several transitions (cf. Fig. 4). The detailed analysis of the first part is based on a curve fitting of line 33, which consists of two components. The dominating part of this line reflects transitions to the $3p^4(^3P)5p\ ^2D_{3/2}$ final state, while transitions to the $3p^4(^3P)5p\ ^2S_{1/2}$ state fall on the low-binding-energy side of the peak [10], making the line asymmetric. Assuming that the relative intensities of the spin-orbit split states follow the statistical ratios, the assignments of the remaining lines are readily made. According to the analysis in Ref. [10], the weak lines labeled 38, 39, 41, and 42 are associated with the spin-orbit-state Ar^{2+} parent states arising from the $3p^4(^3P_{0,1,2})4f$ configuration. Each of these states contains several closely spaced components, which are not resolved in the present study. However, the large splitting between the com-

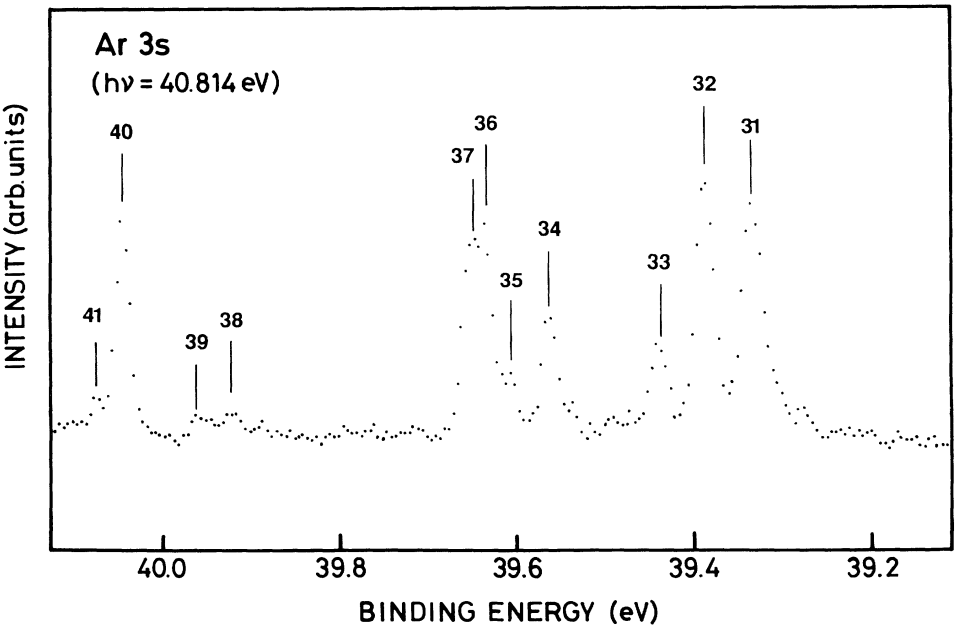

FIG. 4. The He II α excited inner-valence satellite spectrum of argon between 39.2 and 40.1 eV.

ponents associated with the $3p^4(^3P_2)4f$ state gives rise to a doublet structure in the spectrum (lines 38 and 39 in Fig. 4).

In the innermost part of the spectrum, one line (43) at 40.383 eV is well resolved and can be associated with transitions to the $3p^4(^1D)4d\ ^2G_{7/2,9/2}$ states. The remaining lines can be very well fitted using the assignments of Ref. [10], while the alternative assignments of Ref. [9] lead to a strong disagreement with the experimental spectrum under the assumption that the relative intensities between the spin-orbit split components follow the statistical ratios. The structures above 40.6 eV are rather diffuse and assignments of these have therefore not been attempted.

IV. DISCUSSION

With the exception of the first line at 29.240, which corresponds to the $3s3p^6\ ^2S_{1/2}$ single-hole state, all He II excited lines have been associated with transitions to doublet states within the $3s^23p^4nl$ configurations. In no case has an assignment in terms of a quartet state been justified. This suggests that the L and S quantum numbers are well defined and agrees with the conclusion of Ref. [10] that the $3s^23p^4$ parent configuration of Ar III does not deviate much from LS coupling.

The relative intensity of the $3s$ line at 29.240 eV is very low, only 50% of the most intense satellite lines (uncorrected for transmission). This contrasts against the x-ray photoelectron spectrum, where the intensity of the $3s$ line is five times the intensity of the highest satellite $3p^4(^1D)3d\ ^2S_{1/2}$ and also against synchrotron-radiation-excited spectra at 58 and 77 eV [7,8]. However, it is somewhat similar to the behavior of synchrotron-radiation excited spectra in the 40-eV region [8]. The very low relative intensity in the $3s$ line can be explained by the presence of a Cooper minimum in the $3s$ ionization cross section, while the rapidly changing photoionization cross section in the 40-eV range [5] also results in a relative enhancement of the satellite lines.

Considering only doublet states, one might expect to observe the first lines above the $3s$ single-hole line, corresponding to the spin-orbit split $3p^4(^3P)4s\ ^2P_{1/2,3/2}$ states at 32.900 and 33.025 eV, respectively [10]. However, no lines can be clearly identified at these positions. On the other hand, the ^1D-coupled Ar^{2+} parent state of the same configuration gives rise to two close-lying lines with high intensities at 34.187 and 34.214 eV, respectively, and the corresponding ^1S-coupled parent state gives rise to the strongest line in the spectrum at 36.504 eV. A similar behavior is observed for the $3p^45s$ configuration; the ^3P-coupled parent state is completely missing, whereas the ^1D-coupled state gives a substantial intensity. (The ^1S coupled state is expected to occur at 42.424 eV [10], and is thus not observable in the present study.) These observations are consistent with an ISCI-FISCI model (initial-state and final-ionic-state configuration interaction), where the only available final states are ^2S, $^2P^o$, ^2D, $^2F^o$, and ^2G. The ^3P-coupled parent state has even parity and can thus not be involved in transitions to a $3p^44s$ configuration. However, the states are clearly observed in the fluorescence spectrum [11] and also in threshold or near-threshold spectra [2,3], where other selection rules apply.

As mentioned above, the first satellite lines actually observed in the spectrum (lines 2 and 3 of Table I and Fig. 2) correspond to the lowest states, $^2P_{1/2,3/2}$, of the $3p^4(^3P)3d$ configuration. The other states of this configuration, $^2F_{5/2,7/2}$ and $^2D_{3/2,5/2}$ are clearly observed (lines 6,7 and 8,9, respectively), the latter having comparatively high intensity. The corresponding states of the $3p^44d$ configuration are also observed (line pairs 29,30 and 31,32 and 36,37, respectively) with about the same relative intensities as in the $3p^43d$ configuration, as might be expected in a model involving ISCI and FISCI. Surprisingly, the lines 2 and 3 were not observed in the fluorescence spectrum [11], while the corresponding $3p^4(^3P)4d\ ^2P$ lines were observed with intensities relative to the $4d\ ^2D$ lines that are similar to the present result.

Line 10 is associated with the first state, $^2G_{7/2,9/2}$, in the $3p^4(^1D)3d$ configuration. All other components of this configuration are present in the spectrum and correspond to lines 16 ($^2F_{5/2,7/2}$), 20 and 21 ($^2D_{3/2,5/2}$), 24 and 25 ($^2P_{1/2,3/2}$) and 28 ($^2S_{1/2}$). As in the ^3P-coupled parent states, the intensity is quite low for the ^2F states, and also for the ^2G states, as would be expected in an ISCI description where these states require the inclusion of high quantum numbers in the configurations.

The line pair 11 and 12 at 35.440 and 35.522 eV, respectively, corresponds to the $3p^4(^3P)4p\ ^2D_{5/2,3/2}$ states. The remaining states $^2P_{1/2,3/2}$ and $^2S_{1/2}$ are also observed (lines 13, 14, and 15) with rather high intensities, which implies that both ISCI and FISCI should be considered in these cases, as has been found earlier [16]. Among the ^1D-coupled parent states of the same configuration, namely $^2F_{7/2,9/2}$ (lines 18 and 19), $^2P_{1/2,3/2}$ (lines 20 and 21), and $^2D_{3/2,5/2}$ (lines 22 and 23), the ^2D states have very low intensity. This agrees essentially with the expectation for an ISCI-FISCI model, where the transitions to this state are parity forbidden in the LS description.

The $3p^4(^3P)5p\ ^2D_{5/2,3/2}$, $^2P_{1/2,3/2}$, and $^2S_{1/2}$ states are observed above 39 eV (lines 31, 32, and 33), that is, in an energy range less than 2 eV from threshold. Nevertheless, the intensity ratios are not very much different from those of the $3p^4(^3P)4p$ configuration.

The line at 40.383 eV corresponds to the $3p^4(^1D)4d\ ^2G_{7/2,9/2}$ states, which are expected to acquire some intensity in parallel with the observations for the $3p^4(^1D)3d\ ^2G_{7/2,9/2}$ states at 34.877 eV. Also the high-angular-momentum $3p^4(^1D)4d\ ^2F_{7/2,5/2}$ states appearing at 40.573 and 40.585 eV have a considerable intensity, but this is in contrast to the $3p^4(^1D)3d\ ^2F_{7/2,5/2}$ states, which are comparatively weak. This might suggest that at these very low photoelectron energies, only a few tenths of an eV, continuum effects are important as is also seen in threshold spectra [2,3,5].

V. CONCLUSIONS

The inner-valence-photoelectron spectrum of argon has been studied using monochromatized He II α radiation. A large number of previously unresolved states

have been observed and assigned in terms of electron correlation states arising from $3p^4nl$ configurations, where $n=3,4,5$ and $l=0-3$. In most cases, the whole manifold of states arising from the different configurations has been identified. The relative intensities between the lines show that *LS* coupling is appropriate for a description of these states. Except at very low photoelectron energies (below 0.3 eV), the spectrum can be well explained in terms of initial-state and final-ionic-state configuration interaction. Since the theoretical studies so far have concerned primarily the predominant transitions studied at somewhat higher energies no detailed comparison can be made with calculated results. We therefore hope that this study will provide useful data for additional theoretical investigations on the photoionization of argon in the 40-eV region.

[1] S. Svensson, B. Eriksson, N. Mårtensson, G. Wendin, and U. Gelius, J. Electron Spectrosc. **47**, 327 (1988).
[2] R. I. Hall, L. Avaldi, G. Dawber, P. M. Putter, M. A. MacDonald, and G. C. King, J. Phys. B **22**, 3205 (1989).
[3] A. A. Wills, A. A. Cafolla, F. J. Curell, J. Comer, A. Svensson, and M. A. MacDonald, J. Phys. B **22**, 3217 (1989).
[4] M. O. Krause, S. B. Whitfield, C. D. Caldwell, J.-Z. Wu, P. van der Meulen, C. A. de Lange, and R. W. C. Hansen, J. Electron Spectrosc. **58**, 79 (1992).
[5] U. Becker, B. Langer, H. G. Kerkhoff, M. Kupsch, D. Szostak, R. Wehlitz, P. A. Heimann, S. H. Liu, D. W. Lindle, T. A. Ferrett, and D. A. Shirley, Phys. Rev. Lett. **60**, 1490 (1985).
[6] C. E. Brion, A. O. Bawagan, and K. H. Tan, Can. J. Chem. **66**, 1877 (1988).
[7] M. Y. Adam, F. Wuilleumier, S. Krummacher, V. Schmidt, and W. Mehlhorn, J. Phys. B **11**, L413 (1978).
[8] M. Y. Adam, P. Morin, and G. Wendin, Phys. Rev. A **31**, 1426 (1985).
[9] C. E. Moore, *Atomic Energy Levels,* Natl. Bur. Stand. (U.S.) Circ. No. 467 (U.S. GPO, Washington, DC, 1949).
[10] L. Minnhagen, Ark. Fys. **25**, 203 (1963); J. Opt. Soc. Am. **61**, 1257 (1971).
[11] J. A. R. Samson, Y. Chung, and Eun-Mee Lee, Phys. Lett. A **127**, 171 (1988).
[12] R. L. Martin, S. P. Kowalczyk, and D. A. Shirley, J. Chem. Phys. **68**, 3829 (1978).
[13] K. G. Dyall and F. P. Larkins, J. Electron Spectrosc. **15**, 165 (1979).
[14] K. G. Dyall and F. P. Larkins, J. Phys. B **15**, 203 (1982); **15**, 219 (1982).
[15] H. Smid and J. E. Hansen, Phys. Rev. Lett. **52**, 2138 (1984).
[16] W. T. Silvfast, D. Y. Al-Salameh, and O. R. Wood II, Phys. Rev. A **34**, 5164 (1986).
[17] W. Wijesundera and H. P. Kelly, Phys. Rev. A **36**, 4539 (1987).
[18] W. Wijesundera and H. P. Kelly, Phys. Rev. A **39**, 634 (1989).
[19] P. Baltzer, B. Wannberg, and M. C. Göthe, Rev. Sci. Instrum. **62**, 643 (1991); P. Baltzer, L. Karlsson, M. Lundqvist, and B. Wannberg, Rev. Sci. Instrum. **64**, 2179 (1993).
[20] P. Baltzer and L. Karlsson, Uppsala University, Institute of Physics Report No. UUIP-1211, 1989 (unpublished).
[21] P. Baltzer and L. Karlsson, Phys. Rev. A **38**, 2322 (1988).
[22] P. Baltzer, B. Wannberg, M. Carlsson Göthe, and L. Karlsson, Rev. Sci. Instrum. **62**, 630 (1991).
[23] R. P. Madden, D. L. Ederer, and K. Codling, Phys. Rev. **177**, 136 (1968).